Cell Reports, Volume *32*

Supplemental Information

Altered MICOS Morphology and Mitochondrial Ion Homeostasis Contribute to Poly(GR) Toxicity Associated with C9-ALS/FTD

Shuangxi Li, Zhihao Wu, Yu Li, Ishaq Tantray, Diego De Stefani, Andrea Mattarei, Gopinath Krishnan, Fen-Biao Gao, Hannes Vogel, and Bingwei Lu

Supplemental Materials

This file includes:

Supplemental Figures S1 to S4

Legends for Supplemental Figures S1 to S4

Figure S1

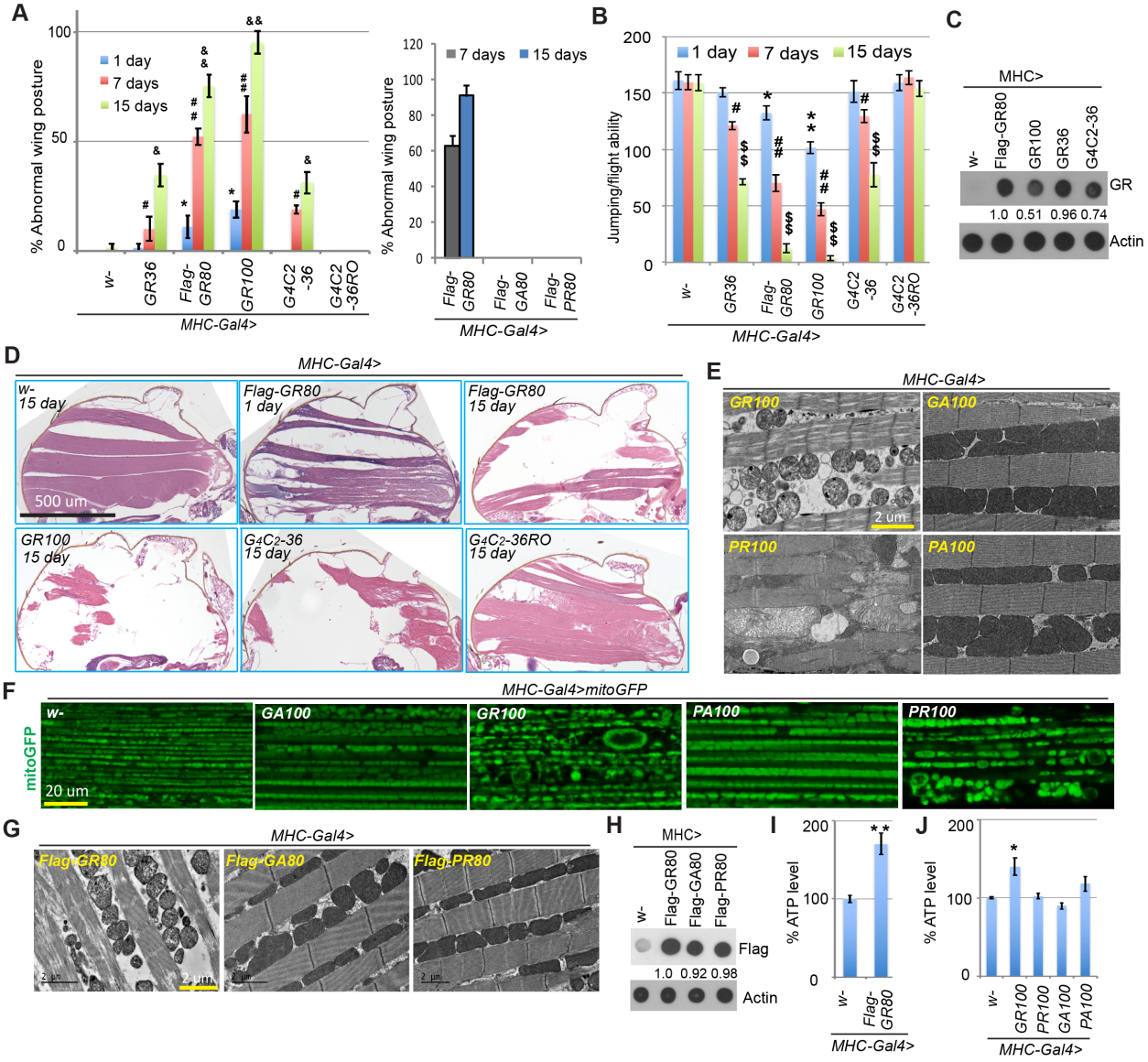
A
% Abnormal wing posture
1 day
7 days
15 days
w-
GR36
Flag-GR80
GR100
G4C2-36
G4C2-36RO
MHC-Gal4>
% Abnormal wing posture
7 days
15 days
Flag-GR80
Flag-GA80
Flag-PR80
MHC-Gal4>
B
Jumping/flight ability
1 day
7 days
15 days
w-
GR36
Flag-GR80
GR100
G4C2-36
G4C2-36RO
MHC-Gal4>
C
MHC>
w-
Flag-GR80
GR100
GR36
G4C2-36
GR
1.0 0.51 0.96 0.74
Actin
D
MHC-Gal4>
w-
15 day
500 um
Flag-GR80
1 day
Flag-GR80
15 day
GR100
15 day
G4C2-36
15 day
G4C2-36RO
15 day
E
MHC-Gal4>
GR100
GA100
2 um
PR100
PA100
F
MHC-Gal4>mitoGFP
mitoGFP
w-
20 um
GA100
GR100
PA100
PR100
G
MHC-Gal4>
Flag-GR80
Flag-GA80
Flag-PR80
H
MHC>
w-
Flag-GR80
Flag-GA80
Flag-PR80
Flag
1.0 0.92 0.98
Actin
I
% ATP level
w-
Flag-GR80
MHC-Gal4>
J
% ATP level
w-
GR100
PR100
GA100
PA100
MHC-Gal4>

Figure S1. Analyses of transgenic flies expressing G4C2 repeats, GR or other DPRs, Related to Figure 1.

(A, B) Analyses of wing posture (A) and jumping/flight ability (B) of the various transgenic flies (n=30 males in A and 10 males in B; 3 biological repeats).

(C) Dot blots quantifying GR expression in the various transgenic fly lines.

(D) H&E staining of paraffin sections of thoracic muscle showing effect of various transgene expression on indirect flight muscle integrity in the corresponding genotypes shown in A.

(E) TEM images of IFM mitochondrial morphology in the various transgenic flies.

(F) Monitoring of mitochondrial morphology in thoracic muscle of various transgenic flies co-expressing a mito-GFP reporter.

(G) TEM images of IFM mitochondrial morphology in transgenic flies expressing Flag-tagged GR80, GA80, and PR80.

(H) Dot blots quantifying Flag-tagged GR80, GA80, and PR80 expression in the transgenic fly lines.

(I, J) Quantification showing increased ATP level in *GR80* (I) and *GR100* (J) flies. (n=30 flies, 4 biological repeats).

*, #, &, and $ indicate $p<0.05$; **, ##, &&, and $$ indicate $p<0.01$ in one-way ANOVA test followed by Student–Newman–Keuls test (SNK test) plus Bonferroni correction. Immunoblots are representative of at least two independent repeats. Images in D-G are representative of three independent samples.

Figure S2

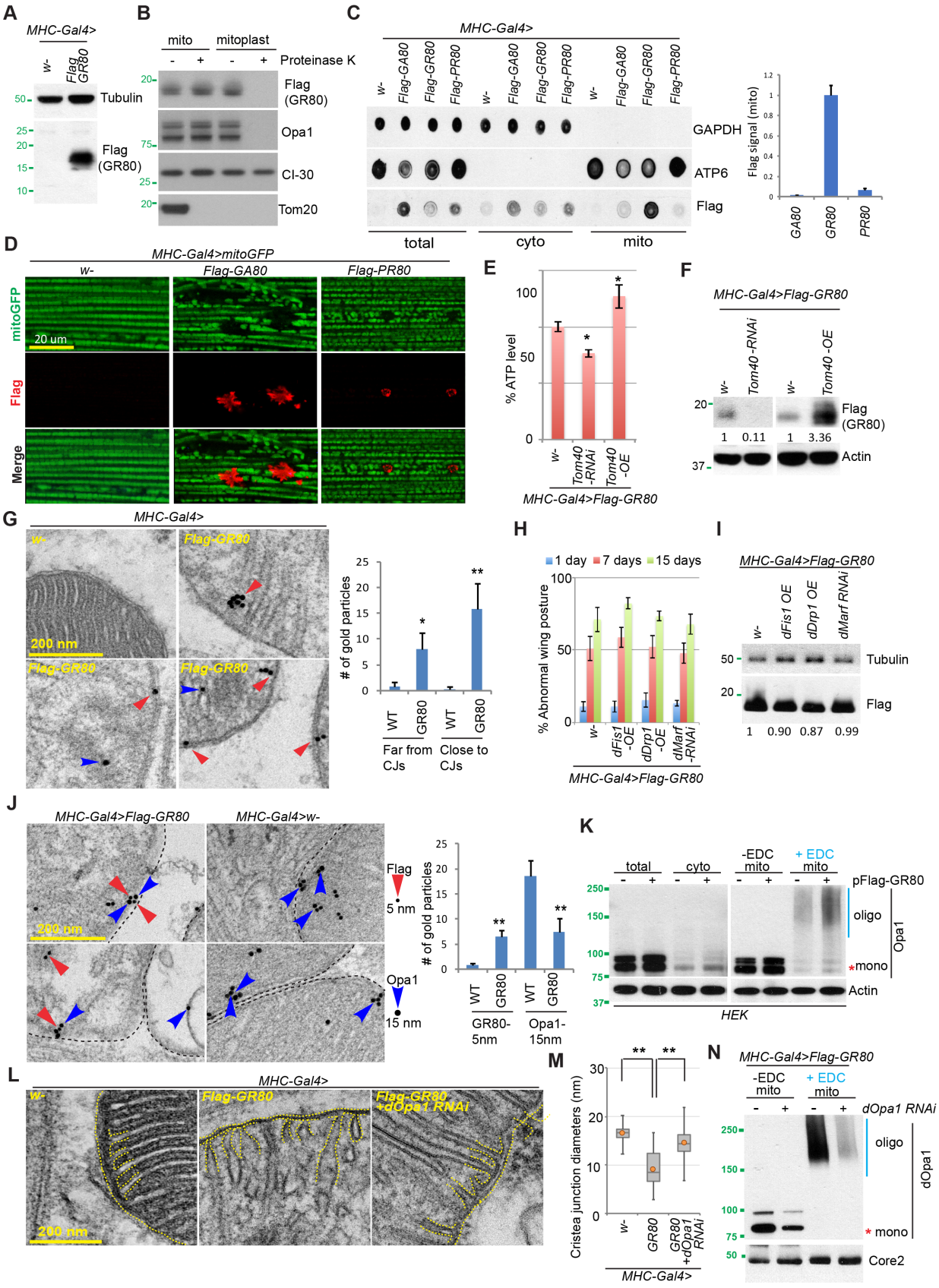
A
MHC-Gal4>
w-
Flag GR80
Tubulin
Flag (GR80)
B
mito
mitoplast
Proteinase K
Flag (GR80)
Opa1
Cl-30
Tom20
C
MHC-Gal4>
w-
Flag-GA80
Flag-GR80
Flag-PR80
GAPDH
ATP6
Flag
total
cyto
mito
Flag signal (mito)
GA80
GR80
PR80
D
MHC-Gal4>mitoGFP
w-
Flag-GA80
Flag-PR80
mitoGFP
Flag
Merge
20 um
E
% ATP level
w-
Tom40 -RNAi
Tom40 -OE
MHC-Gal4>Flag-GR80
F
MHC-Gal4>Flag-GR80
w-
Tom40 -RNAi
Tom40 -OE
Flag (GR80)
Actin
1 0.11 1 3.36
G
MHC-Gal4>
w-
Flag-GR80
200 nm
# of gold particles
WT
GR80
Far from CJs
Close to CJs
H
1 day
7 days
15 days
% Abnormal wing posture
w-
dFis1 -OE
dDrp1 -OE
dMarf -RNAi
MHC-Gal4>Flag-GR80
I
MHC-Gal4>Flag-GR80
w-
dFis1 OE
dDrp1 OE
dMarf RNAi
Tubulin
Flag
1 0.90 0.87 0.99
J
MHC-Gal4>Flag-GR80
MHC-Gal4>w-
200 nm
Flag
5 nm
Opa1
15 nm
# of gold particles
WT
GR80
GR80-5nm
Opa1-15nm
K
total
cyto
-EDC mito
+ EDC mito
pFlag-GR80
oligo
*mono
Opa1
Actin
HEK
L
MHC-Gal4>
w-
Flag-GR80
Flag-GR80 +dOpa1 RNAi
200 nm
M
Cristea junction diameters (nm)
w-
GR80
GR80 +dOpa1 RNAi
MHC-Gal4>
N
MHC-Gal4>Flag-GR80
-EDC mito
+ EDC mito
dOpa1 RNAi
oligo
* mono
dOpa1
Core2

Figure S2. Additional analysis of the mitochondrial localization and Opa1 interaction of GR80, Related to Figure 2.

(A) Immunoblots showing robust expression of Flag-GR80 in fly thoracic muscle extract from *GR80* flies. Tubulin serves as loading control.

(B) Proteinase K sensitivity assay of intact mitochondria and mitoplasts showing similar behavior of GR80 and IMS-facing Opa1.

(C) Dot blots showing the presence of GR80, but not GA80 or PR80, in the mitochondrial fraction prepared from thoracic muscle of transgenic flies. GAPDH serves as cytosolic marker; mt:ATP6 serves as mitochondrial marker. The residual Flag signals in Flag-GA80 and Flag-PR80 mitochondrial fractions are largely background signals. Graph shows quantification (n=3).

(D) Immunostaining showing lack of mitochondrial localization of Flag-GA80 or Flag-PR80 in fly thoracic flight muscle expressing a mito-GFP reporter. Images are representative of three independent samples.

(E) Bar graph showing quantification of the effect of Tom40 RNAi or OE on ATP level in *GR80* flies (n=4).

(F) Immunoblots showing the effect of Tom40 RNAi or OE on GR80 protein level in fly thoracic muscle.

(G) Immune-EM images showing mitochondrial localization of Flag-GR80 in fly thoracic muscle. Arrowheads indicate GR80 localized to the matrix (blue) or close to the cristae (red). Graph shows quantification (n=4).

(H, I) Lack of obvious effect on wing posture (H) or GR80 protein expression (I) by genetic manipulation of mitochondrial fission or fusion related proteins (n=3).

(J) Double-label immune-EM analysis of Flag-GR80 and Opa1 co-localization on mitochondrial membrane in fly thoracic muscle. Red and blue arrows mark Flag-GR80 and Opa1 signals, respectively, labeled with different sized gold particles. Graph shows quantification (n=4).

(K) Immunoblots showing effect of Flag-GR80 expression on Opa1 oligomer formation in HEK293T cells. EDC was used to cross-link Opa1 proteins. The positions of Opa1 monomers and oligomers are indicated.

(L-N) Effect of Opa1 RNAi on CJ morphology (L), CJ diameter (M), or Opa1 oligomer formation (N) in *GR80* thoracic muscle (n=22~25 CJs analyzed, 3 biological repeats for M).

* and ** indicate $p<0.05$ and $P<0.01$ in one-way ANOVA test followed by Student–Newman–Keuls test (SNK test) plus Bonferroni correction. Data in M was analyzed and presented by the Box-and-Whisker Plot. **, $p<0.01$. Immunoblots are representative of at least two independent repeats.

Figure S3

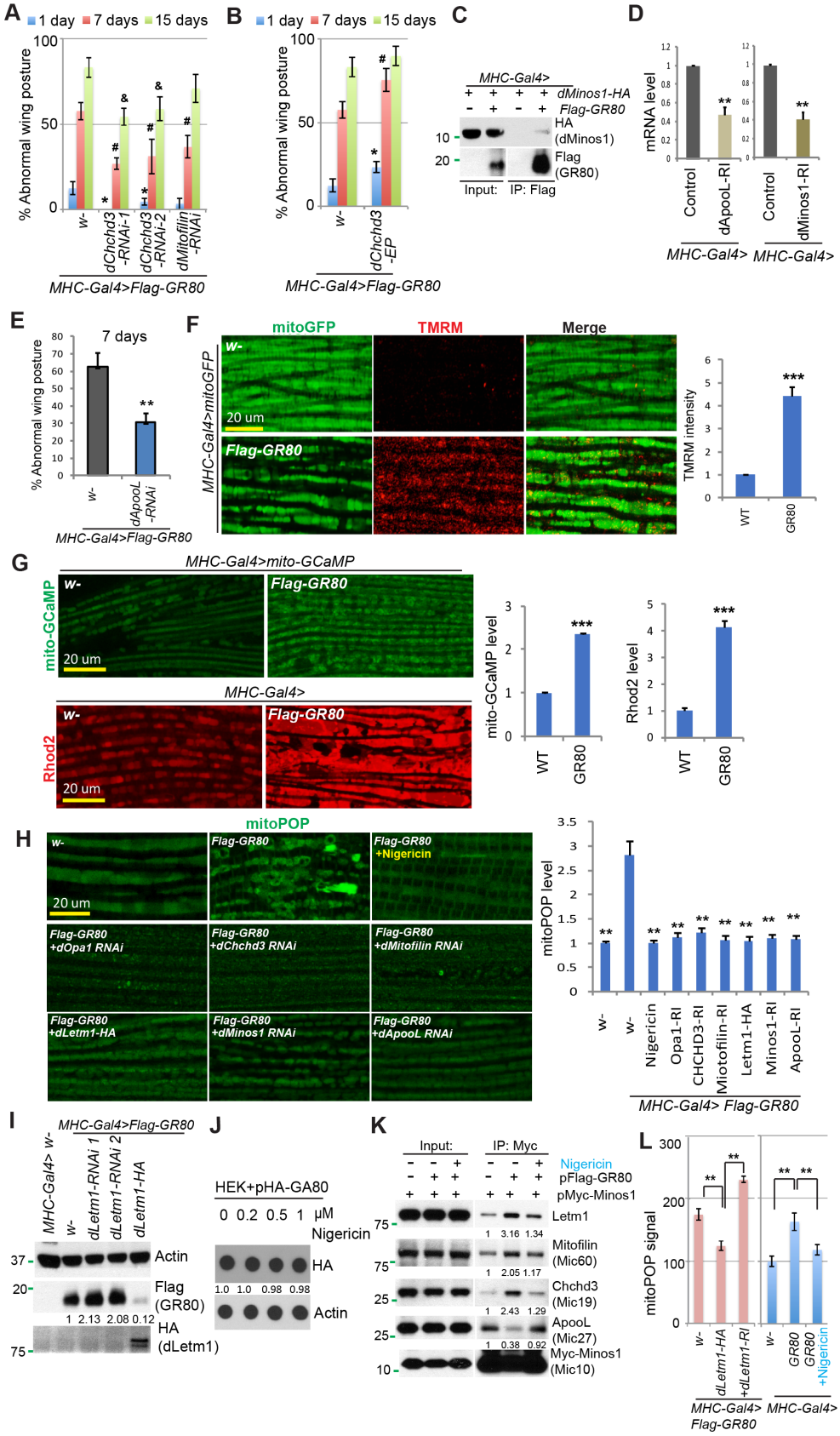
A
1 day
7 days
15 days
% Abnormal wing posture
w-
dChchd3 -RNAi-1
dChchd3 -RNAi-2
dMitofilin -RNAi
MHC-Gal4>Flag-GR80
B
dChchd3 -EP
C
MHC-Gal4>
dMinos1-HA
Flag-GR80
HA (dMinos1)
Flag (GR80)
Input:
IP: Flag
D
mRNA level
Control
dApooL-RI
dMinos1-RI
E
7 days
dApooL -RNAi
F
mitoGFP
TMRM
Merge
MHC-Gal4>mitoGFP
20 um
Flag-GR80
TMRM intensity
WT
GR80
G
MHC-Gal4>mito-GCaMP
mito-GCaMP
MHC-Gal4>
Rhod2
mito-GCaMP level
Rhod2 level
H
mitoPOP
Flag-GR80 +Nigericin
Flag-GR80 +dOpa1 RNAi
Flag-GR80 +dChchd3 RNAi
Flag-GR80 +dMitofilin RNAi
Flag-GR80 +dLetm1-HA
Flag-GR80 +dMinos1 RNAi
Flag-GR80 +dApooL RNAi
mitoPOP level
Nigericin
Opa1-RI
CHCHD3-RI
Miotofilin-RI
Letm1-HA
Minos1-RI
ApooL-RI
I
MHC-Gal4>Flag-GR80
dLetm1-RNAi 1
dLetm1-RNAi 2
dLetm1-HA
Actin
Flag (GR80)
HA (dLetm1)
J
HEK+pHA-GA80
0 0.2 0.5 1 μM Nigericin
HA
Actin
K
Input:
IP: Myc
Nigericin
pFlag-GR80
pMyc-Minos1
Letm1
Mitofilin (Mic60)
Chchd3 (Mic19)
ApooL (Mic27)
Myc-Minos1 (Mic10)
L
mitoPOP signal
dLetm1-HA
dLetm1-RI
GR80
GR80 +Nigericin

Figure S3. Additional data on GR80 effects on MICOS and mitochondrial ion homeostasis, Related to Figure 3.

(A, B) Bar graphs showing quantification of the effects of RNAi-mediated knockdown of CHCHD3 and mitofilin (A) or OE of CHCHD3 with an EP line (B) on wing posture in *GR80* flies (n=90 flies analyzed, 3 biological repeats).

(C) Immunoblots showing Co-IP between Flag-GR80 and Minos1-HA in fly muscle.

(D) Quantification of mRNA level by qRT-PCR showing the knockdown efficiency of the respective RNAi lines (n=3).

(E) Bar graph showing quantification of the effect of Mic27 (Apool) RNAi on the wing-posture phenotype of *GR80* flies (n=3).

(F) Confocal images showing TMRM staining of MMP in *GR80* fly muscle. Graph shows quantification (n=6).

(G) Images showing mito-Ca^{2+} levels in *GR80* fly muscle monitored using mito-GCaMP reporter or Rhod2-AM dye. Graphs show quantification (n=3).

(H) Images showing mito-K^{+} level monitored using mito-POP in *GR80* fly muscle after nigericin treatment or after genetic manipulation of MICOS components. Graph shows quantification (n=3).

(I) Immunoblots showing effects of knockdown or OE of LETM1 on GR80 protein expression in fly thoracic muscle.

(J) Dot blot showing lack of effect of nigericin on GA80 level in HEK293 cells.

(K) Immunoblots showing effect of nigericin treatment on the interaction between Minos1 and MICOS components in transfected HEK293T cells.

(L) Bar graph showing quantification of mito-K^+ level in purified mitochondria from *GR80* fly muscle with or without genetic manipulation of LETM1 (left) or with or without nigericin treatment (right) (n=3).

*, #, &, and $ indicate $p<0.05$; ** and *** indicate $p<0.01$ and $P<0.001$, respectively, in one-way ANOVA test followed by Student–Newman–Keuls test (SNK test) plus Bonferroni correction. Immunoblots are representative of at least two independent repeats.

Figure S4

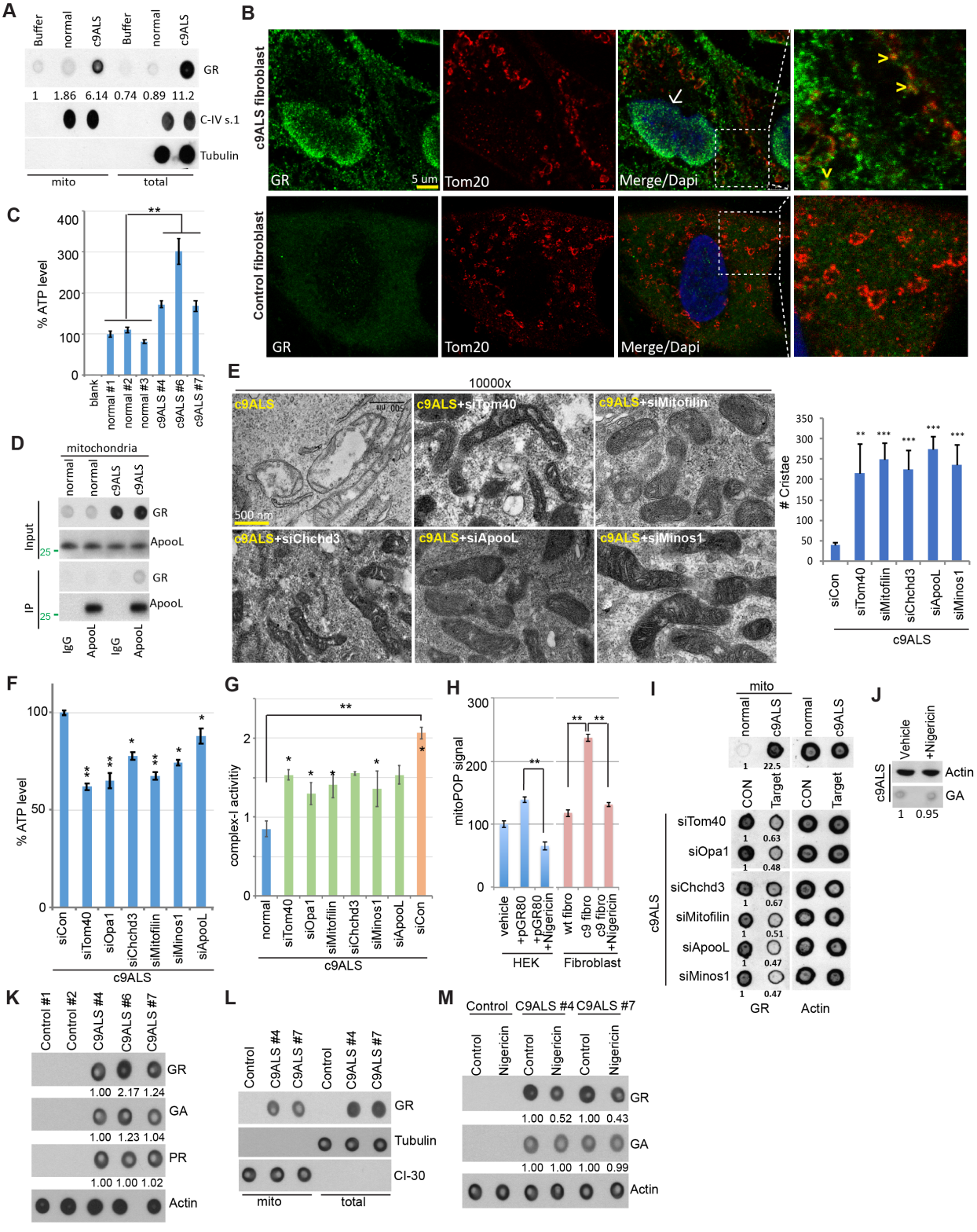
A
Buffer
normal
c9ALS
Buffer
normal
c9ALS
GR
1 1.86 6.14 0.74 0.89 11.2
C-IV s.1
Tubulin
mito
total
B
c9ALS fibroblast
Control fibroblast
GR
5 um
Tom20
Merge/Dapi
C
% ATP level
blank
normal #1
normal #2
normal #3
c9ALS #4
c9ALS #6
c9ALS #7
D
mitochondria
Input
IP
GR
ApooL
IgG
ApooL
E
10000x
c9ALS
c9ALS+siTom40
c9ALS+siMitofilin
c9ALS+siChchd3
c9ALS+siApooL
c9ALS+siMinos1
500 nm
Cristae
siCon
siTom40
siMitofilin
siChchd3
siApooL
siMinos1
c9ALS
F
% ATP level
siCon
siTom40
siOpa1
siChchd3
siMitofilin
siMinos1
siApooL
c9ALS
G
complex-I activity
normal
siTom40
siOpa1
siMitofilin
siChchd3
siMinos1
siApooL
siCon
c9ALS
H
mitoPOP signal
vehicle
+pGR80
+pGR80 +Nigericin
wt fibro
c9 fibro
c9 fibro +Nigericin
HEK
Fibroblast
I
mito
normal
c9ALS
normal
c9ALS
1 22.5
CON
Target
CON
Target
siTom40
1 0.63
siOpa1
1 0.48
siChchd3
1 0.67
siMitofilin
1 0.51
siApooL
1 0.47
siMinos1
1 0.47
c9ALS
GR
Actin
J
c9ALS
Vehicle
+Nigericin
Actin
GA
1 0.95
K
Control #1
Control #2
C9ALS #4
C9ALS #6
C9ALS #7
GR
1.00 2.17 1.24
GA
1.00 1.23 1.04
PR
1.00 1.00 1.02
Actin
L
Control
C9ALS #4
C9ALS #7
Control
C9ALS #4
C9ALS #7
GR
Tubulin
CI-30
mito
total
M
Control
C9ALS #4
C9ALS #7
Control
Nigericin
Control
Nigericin
Control
Nigericin
GR
1.00 0.52 1.00 0.43
GA
1.00 1.00 1.00 0.99
Actin

Figure S4. Effect of genetic manipulation of MICOS components on mitochondrial defects in C9ALS patient fibroblasts, Related to Figure 4.

(A) Dot blot assay analyzing GR peptide expression in the mitochondria of C9ALS patient fibroblasts. Complex-IV, subunit 1 (C-IV s.1) serves as mitochondrial marker, tubulin as cytosolic marker.

(B) Immunostaining showing GR expression in patient fibroblasts and its localization to mitochondrial and nuclear compartments. Arrowhead and arrow mark mitochondrial and nuclear signals of GR, respectively. Images are representative of three independent samples.

(C) Quantification of ATP level in normal and C9ALS patient fibroblasts (n=3).

(D) Co-IP assay showing Apool/GR interaction in patient fibroblasts. Apool is detected by standard western blot, GR by dot blot.

(E) TEM images showing aberrant mitochondrial morphology in C9ALS patient fibroblasts and the effect of siRNA-mediated knockdown of various MICOS components in rescuing the cristae loss phenotype of patient cells. Graph shows quantification (n=10, 3 biological repeats).

(F) Quantification of ATP level in C9ALS fibroblasts showing effects of siRNA-mediated knockdown of various MICOS components. Scrambled siRNA (siCON) serves as control (n=3).

(G) Measurements of complex-I activity in C9ALS fibroblasts showing effects of siRNA-mediated knockdown of various MICOS components (n=3).

(H) Measurement of mito-K^+ level in purified mitochondria from HEK293T cells transfected with GR80 and treated with nigericin or LETM1 siRNA, or from control and C9ALS fibroblasts with or without nigericin treatment (n=4).

(I) Dot blot analysis showing effects siRNA-mediated knockdown of various MICOS components on GR peptide expression. Actin serves as loading control.

(J) Dot blot assay showing lack of effect of nigericin on GA level in patient fibroblasts.

(K) Dot blot assays showing the co-existence of GR, GA, and PR in three independent patient fibroblast cell lines. Note that line #6 is used in most experiments. Actin serves as loading control.

(L) Dot blot assays showing the presence of GR in the mitochondrial fraction of additional patient fibroblast cell lines #4 and #7. C-I30 and tubulin serve as mitochondrial and cytosolic markers.

(M) Dot blot assays showing the reduction of GR but not GA level by nigericin treatment in additional patient fibroblast cell lines #4 and #7. Actin serves as loading control.

*, **, and *** indicate $p<0.05$, $p<0.01$ and $P<0.001$, respectively, in one-way ANOVA test followed by Student–Newman–Keuls test (SNK test) plus Bonferroni correction. Immunoblots are representative of at least two independent repeats.